

Chapter 16

Role of Fungi in the Removal of Heavy Metals and Dyes from Wastewater by Biosorption Processes



Ajay Kumar, Vineet Kumar, and Joginder Singh

16.1 Introduction

World population is increasing day by day; hence, to meet the demand of the growing population, clean water is the major concern. Water is being polluted by human activities and industrial discharges. These pollutants are categorized into three major groups: organic, inorganic, and biological particles. Heavy metals and dyes as waste from various industries including textile, pharmaceutical, leather, etc. are the major pollutant present in water (Burakov et al. 2018). Heavy metal ions are elements from the fourth period of the periodic table, mostly chromium (Cr), cobalt (Co), nickel (Ni), copper (Cu), zinc (Zn), arsenic (As), lead (Pb), and mercury (Hg). Removing heavy metals is necessary because they are toxic substances with carcinogenic nature that should not to be discharged directly into the environment. Conventional techniques like membrane separation, precipitation, coagulation, and flocculation are widely used for removal of heavy metals (Azimi et al. 2017; Marzougui et al. 2017). Biosorption is preferred over these conventional techniques due to high affinity, capacity, and selectivity of the materials from the solution. There are different mechanisms involved in biosorption phenomenon (Fig. 16.1). There are different kinds of adsorbent available for wastewater treatment. Adsorbents are broadly classified into conventional and nonconventional. Biosorbents are nonconventional adsorbents and have several advantages over other conventional and nonconventional methods (Fig. 16.2).

Microorganism is one type of biosorbents that has been used for wastewater treatment. Many living or dead microorganisms such as bacteria, fungus, and

A. Kumar (✉) · V. Kumar
School of Bioengineering and Biosciences, Lovely Professional University,
Phagwara, Punjab, India

J. Singh
Department of Biotechnology, School of Bioengineering and Biosciences,
Lovely Professional University, Jalandhar, Phagwara, Punjab, India

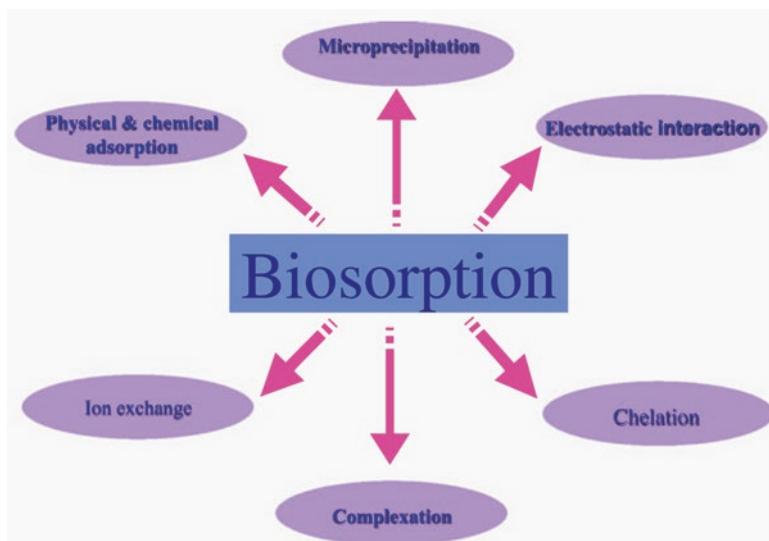


Fig. 16.1 Different mechanisms involved in biosorption phenomenon (Asgher 2012)

algae are widely used for heavy metal removal because of high adsorption capacity, low cost, and its availability in large quantities (Kour et al. 2019a; Rastegari et al. 2019). However, it suffers from some of the drawbacks like waste may be converted into more potential toxic compounds. Most of the microorganism-based methods deal with discoloration of dye instead of removal of dye or other wastes. Dyes are mostly used in textile, leather, and pharmaceutical industries. Discharge of dyes directly into the water bodies causes threats to aquatic fauna and flora as it interferes with gas solubility. Higher concentration of dyes resulted in carcinogenicity and toxicity. Use of fungi for wastewater treatment is one of the promising alternative to physical and chemical process (Couto 2009; Yadav et al. 2016, 2019b). Classification of dyes according to the chemical structure is depicted in Fig. 16.3.

However, nanomaterial-based approaches of wastewater treatment are considered more useful as they allow comparatively better removal of wastewater (Masoudi et al. 2018). With advances in nanotechnology, more and more useful nanomaterials such as graphene, carbon nanotubes, and fullerenes are being produced for wastewater treatment. Along with wastewater treatment, these nanomaterials are also useful for various other environmental applications (Hegab et al. 2018; Nyairo et al. 2018; Park et al. 2017). Figure 16.4 shows nanomaterials used for heavy metal treatment of water. Synthesis of bionanocomposite is now in practice for wastewater treatment. Wang et al. (2018) reported the removal of methylene blue by adsorption on yeast composite assisted with Fe_2O_3 nanoparticles. Figure 16.5 shows the scheme diagram for the synthesis of bio-nanocomposites.

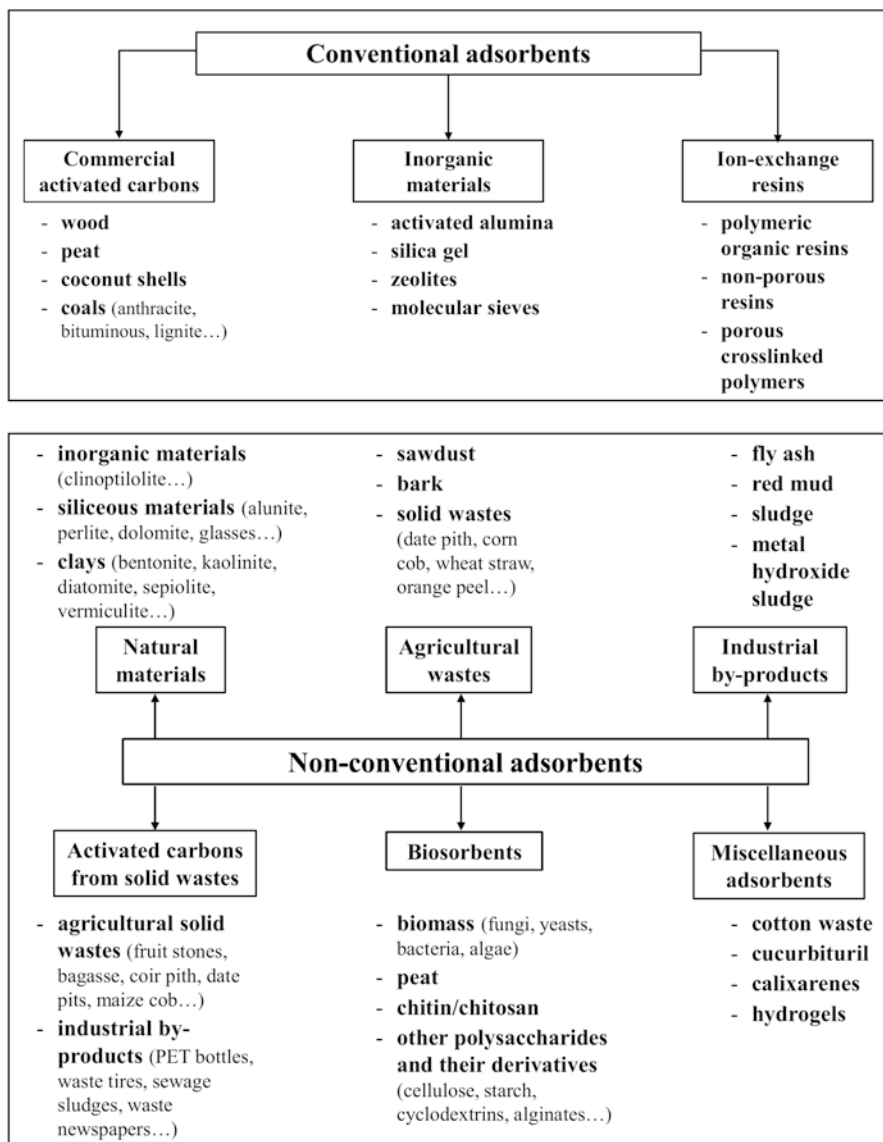


Fig. 16.2 Various methods for wastewater treatment methods (Crini et al. 2018)

16.2 Fungi as Biosorbent

Fungi are osmo-heterotrophic eukaryotes placed in the kingdom *Fungi*. The fungal cell wall is composed of acid polysaccharides such as chitin (a polymer of acetylglucosamine unit), and chitosan, which is characterized by phosphate, amine, and

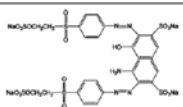
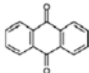
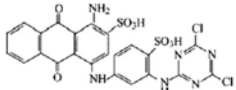
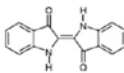
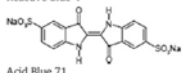
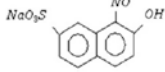
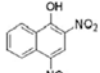
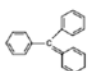
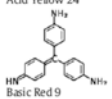
Class	Chromophores	Example
Azo dyes	—N=N—	 Reactive Black 5
Antraquinone dyes		 Reactive Blue 4
Indigoid dyes		 Acid Blue 71
Nitroso dyes	—N=O	 Acid green 1
Nitro dyes	—N(O)_2	 Acid Yellow 24
Triarylmethane dyes		 Basic Red 9

Fig. 16.3 Classification of dyes according to the chemical structure (Yagub et al. 2014)

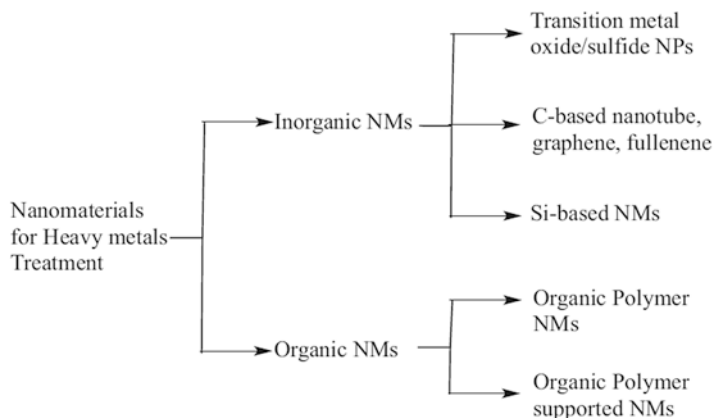


Fig. 16.4 Nanomaterials for heavy metal treatment of water (Lu and Astruc 2018)

hydroxyl groups, is involved in biosorption of heavy metals, dyes, and phenolic compounds (Zhu et al. 2019). They lack chlorophyll and their vegetative structure may be filamentous or unicellular. They reproduce through spore formation (Raghukumar 2017). Figure 16.6 shows the structure of chitin (Fig 16.6a) and chitosan (Fig 16.6b) and their binding with metal ions. Table 16.1 shows the characteristics of major fungal divisions.

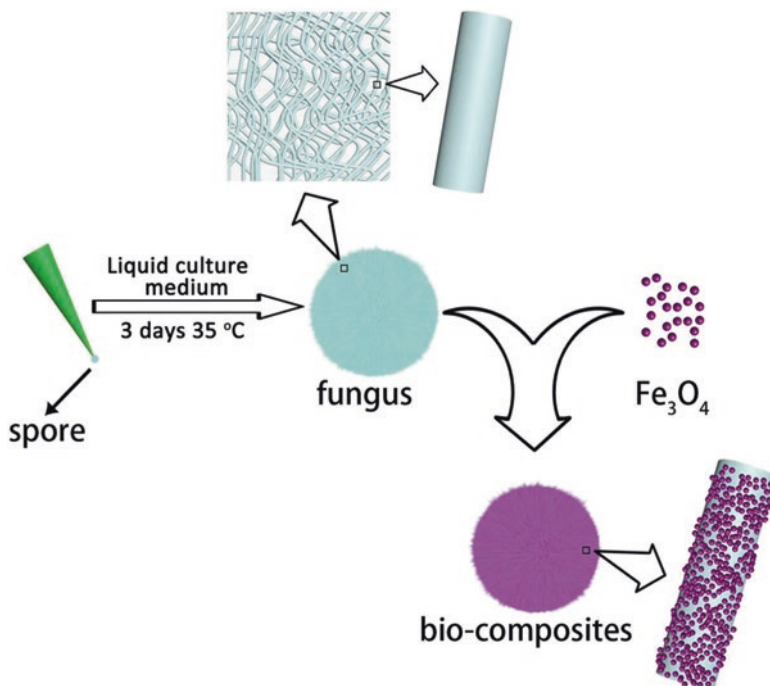


Fig. 16.5 The scheme diagram for the synthesis of bio-nanocomposites

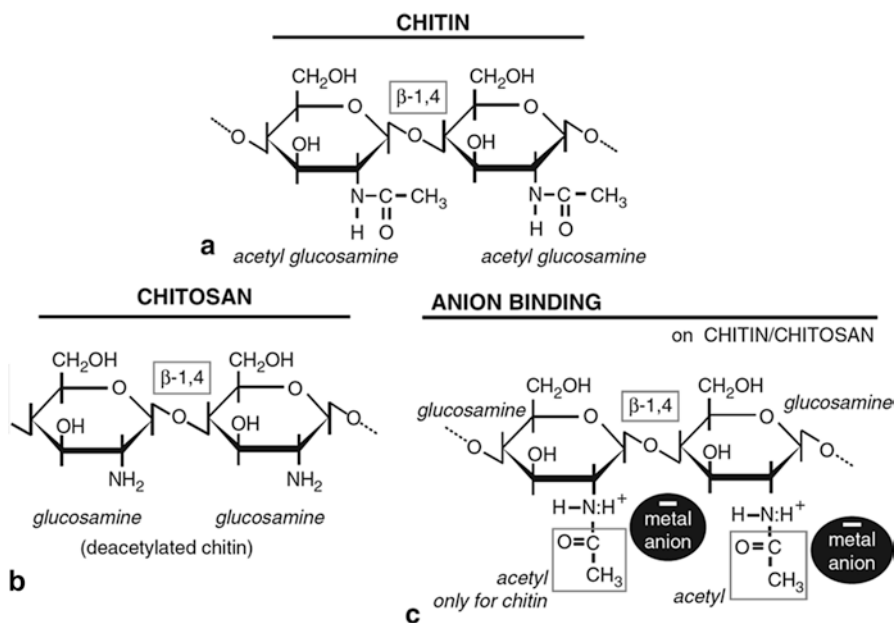


Fig. 16.6 (a) The units of a chitin polymer molecule. (b) Chitosan is deacetylated chitin. (c) Binding of metal anions on chitin or chitosan (Kotrba 2011)

Table 16.1 Characteristics of major fungal divisions (Stajich et al. 2009)

Division	Characteristics
<i>Chytridiomycota</i>	The fungi produce zoospores capable of moving on their own through a liquid medium by simple flagella
<i>Zygomycota</i>	The hyphae do not have one nucleus per cell but rather have long multinucleate, haploid hyphae that comprise their mycelia. Asexual reproduction is by spores produced in stalked sporangia
<i>Ascomycota</i>	They contain more than 30,000 species of unicellular (yeasts) to multicellular fungi. Yeasts reproduce asexually by budding and sexually by forming a sac/ascus
<i>Basidiomycota</i>	Mushrooms, toadstools, and puffballs are commonly encountered basidiomycetes. These conspicuous features of the fungi are the reproductive structures. Sexual reproduction involves the formation of basidiospores on club-shaped cells known as basidia
<i>Deuteromycota</i>	A group of fungi that either lack the perfect stage (i.e., sexual reproduction) or whose perfect stage is as yet undiscovered. They reproduce most frequently by conidia or conidia-like spores. Many forms of deuteromycota are pathogenic, affecting man, animals, or plants

For removal of dyes from wastewater, different forms of fungal sorbents are used such as fungal pellets, mycelium, or dead fungus by many researchers (Yagub et al. 2014). Many molds and filamentous microorganisms such as *Aspergillus niger*, *Penicillium simplicissimum*, *Aspergillus fumigatus*, *Termitomyces clypeatus*, *Penicillium brevicompactum*, *Saccharomyces cerevisiae*, *Trichoderma*, etc. are used for removal of heavy metals and dyes (Rana et al. 2019a, b; Yadav et al. 2019a, b). Fungus can survive in the presence of high metal concentration. So it can be used for heavy metal removal from wastewater. Heavy metal adsorption by fungi through ion exchange and coordination is due to the presence of chitin–chitosan, glucuronic acid, phosphate, and polysaccharides present in/on the cells of fungi. Different kinds of functional groups such as amine, carboxyl, hydroxyl, phosphate, and sulfhydryl play a vital role in the adsorption of heavy metals and dyes by fungal stains (Yin et al. 2018). Fungi especially white-rot fungi and their enzymes (laccase, lignin peroxidase, and Mn peroxidase) can be used to bioremediate various xenobiotics and wastewaters (Kour et al. 2019b; Yadav et al. 2017a, b; 2018). Figure 16.7 shows the schematic diagram of adsorption mechanism model.

16.3 Growth Models for Filamentous Organisms

Fungal biomass can be easily cultivated, or it can be available as industrial waste product such as *Aspergillus niger* (waste from citric acid production) and *Saccharomyces cerevisiae* (brewery industry waste) (Dhankhar and Hooda 2011). At high cell density, filamentous organisms such as molds often form microbial pellets in suspension culture. During the growth process, filamentous organism

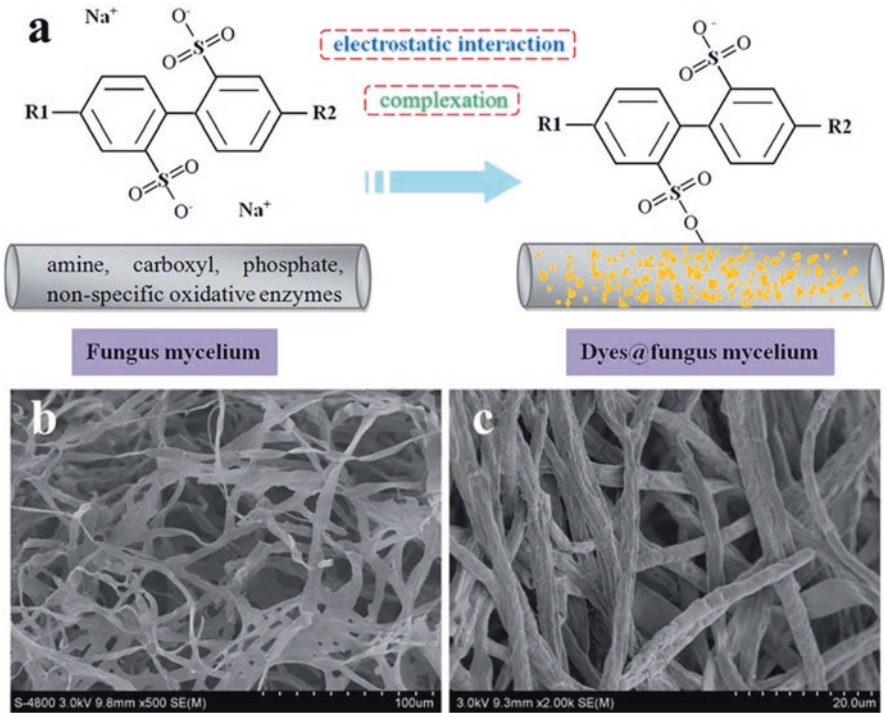


Fig. 16.7 (a) Schematic diagram of adsorption mechanism model. (b) SEM images of fungus mycelia and (c) dyes adsorbed onto fungus mycelia (Li et al. 2019)

increases in their size and mass. Thus, in the absence of mass transfer limitations, the radius of the microbial pellet increases linearly with time.

$$\frac{dR}{dt} = k_p = \text{constant } t \tag{16.1}$$

The growth rate of mold colony can be expressed as follows:

$$\frac{dM}{dT} = \rho 4\pi R^2 \frac{dR}{dt} = k_p 4\pi R^2 \rho \tag{16.2}$$

$$\frac{dM}{dT} = \gamma M^{2/3} \tag{16.3}$$

where $\gamma = k_p(36\pi\rho)^{1/3}$

The mass of spherical pellet as a function of time is given as follows:

$$M = \left(M_0^{1/3} + \frac{\gamma t}{3} \right)^3 \approx \left(\frac{\gamma t}{3} \right)^3 \tag{16.4}$$

where M_0 is the initial mass which is very small as compared with the M and therefore M varies with cubic power with time.

16.4 Surface Modification of Fungal Biomass

Surface modification of biomass is one of the strategies used for adsorption of heavy metals and dyes. Various pretreatment methods such as acid, base, and thermal treatment are used for surface modification of biomass to enhance the adsorption capacity of biomass (Yin et al. 2018) as shown in Fig. 16.8.

16.4.1 Acid Pretreatment

Biomass treated with acid improved the positive charge density on the surface which provide strong electrostatic attraction for negatively charged heavy metal ions.

16.4.2 Base Pretreatment

Biomass treated with alkali may increase negative charge on the surface of biomass to enhance the electrostatic attraction for positively charged heavy metal ions.

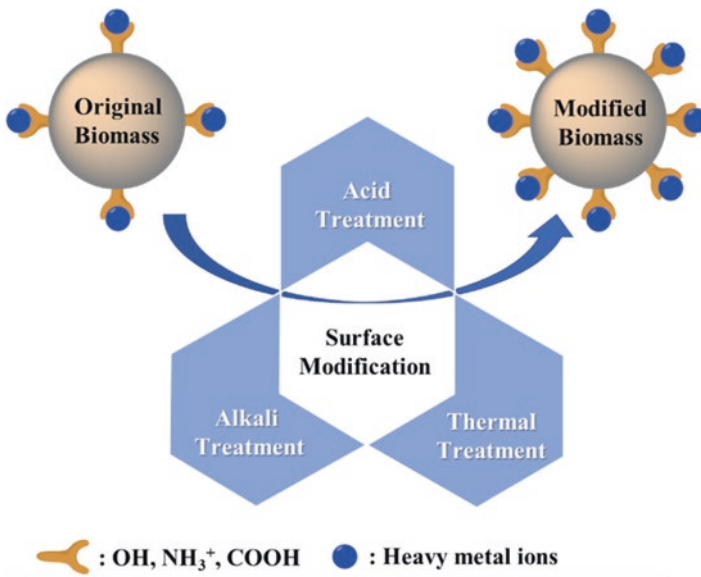


Fig. 16.8 Enhancing heavy metal removing efficiency of biomass through surface modification (Yin et al. 2018)

16.4.3 Thermal Treatment

The porosity and surface area of biomass can be enhanced by thermal treatment for adsorption capacity of biomass. The thermal treatment can also increase the surface functional groups by adding metal-binding groups.

16.5 Biosorption Models and Isotherms

Biosorption is defined as the removal of substance from biological materials whether it is living or dead which involves the phenomenon of the mass transfer. Biosorption involves both the adsorption and absorption processes.

Sorption mechanism can be divided into four consecutive steps:

- (i) Transport of solute in the bulk solution
- (ii) Diffusion of solute through the liquid film surrounding the adsorbent particles
- (iii) Diffusion of solute in the pores of the sorbent (intraparticle diffusion)
- (iv) Chemical reaction as adsorption and desorption on the solid surface

16.5.1 Adsorption Thermodynamics

Thermodynamic behavior of heavy metals and dyes on biosorbent is cited as exothermic or endothermic sorption processes. Free energy gives the information about the physical sorption or chemical sorption (Yao et al. 2010; Madala et al. 2017).

$$\Delta G^\circ = -RT \ln K \quad (16.5)$$

$$\Delta G^\circ = \Delta H^\circ - T\Delta S^\circ \quad (16.6)$$

$$\ln K = \frac{\Delta S^\circ}{R} - \frac{\Delta H^\circ}{RT} \quad (16.7)$$

where ΔG° (J/mol) is Gibb's energy, R is the ideal gas constant (8.314 J/mol K), T is temperature in Kelvin (K), ΔS° (J/mol K) is adsorption entropy, and ΔH (J/mol) is adsorption enthalpy.

K can be obtained from q_e/C_e , while the values of ΔH° and ΔS° were determined from the slope and intercept of the van't Hoff plot of $\ln K$ versus $1/T$.

The negative values of ΔG° suggested the spontaneous behavior of adsorption process. The positive values of ΔH° indicate the endothermic process for the adsorption of metals and dye. The positive value of ΔS° suggested the increasing randomness between the solid and solution interface during the adsorption process.

16.5.2 Adsorption Isotherm

Several mathematical models have been developed by the researchers to validate the process of adsorption (Lei et al. 2018). Kumari and Abraham (2007) describe bio-adsorption of anionic textile dyes by nonviable biomass of fungi and yeast.

The Freundlich model assumes that the adsorbent surface is heterogeneous and sorption on its surface is multilayer.

$$q_e = K_f c_e^{1/n} \quad (16.8)$$

$$\ln q_e = \ln K_f + \frac{1}{n} \ln c_e \quad (16.9)$$

where C_e (mg/L) is the equilibrium concentration in solution, q_e (mg/g) is the lead adsorbed at equilibrium, n is Freundlich constant related to adsorption intensity, and K_f is adsorption constant for Freundlich model.

Thermodynamic parameters of adsorption of silver onto biochar were calculated from Langmuir isotherm as documented by Antunes et al. (2017).

$$q_e = \frac{b q_m c_e}{1 + b c_e} \quad (16.10)$$

The linear form of Langmuir isotherm model equation

$$\frac{C_e}{q_e} = \frac{C_e}{q_m} + \frac{1}{(q_m \cdot b)} \quad (16.11)$$

where c_e (mg/L) is the equilibrium concentration of Cu(II), q_e (mg/g) is the adsorption capacity, q_m (mg/g) is the theoretical maximum sorption capacity, and b (L/mg) is the Langmuir constant related to adsorption energy.

The plot of C_e/q_e against C_e gives a straight line with a slope and intercept of $1/q_m$ and $1/q_m b$, respectively.

The separation factor, R_L , can be determined from Langmuir plot as per the following relation:

$$R_L = \frac{1}{(1 + b C_0)} \quad (16.12)$$

where R_L values indicate the type of adsorption to be irreversible ($R_L = 0$), favorable ($0 < R_L < 1$), linear ($R_L = 1$), or unfavorable ($R_L > 1$), and C_0 is the initial metal or dye concentration (ppm).

The Dubinin–Radushkevich (D-R) equation is described for adsorption nonporous, macroporous, and mesoporous adsorbents. The linear D-R isotherm model equation

$$\ln q_e = \ln q_D - B_D \left[RT \ln \left(1 + \frac{1}{C_e} \right) \right]^2 \quad (6.13)$$

where B_D is related to the free energy of adsorption and q_D is the D-R isotherm constant related to the degree of adsorption by the adsorbent.

The Temkin isotherm is based on the assumption that heat of adsorption would decrease linearly with increase of coverage of adsorbent due to adsorbate/adsorbent interactions.

The linearized Temkin isotherm equation

$$q_e = Q_T \ln K_T + Q_T \ln C_e \quad (6.14)$$

where $Q_T = RT/b_T$, b_T is the Temkin constant related to the heat of adsorption (kJ/mol), K_T is the Temkin isotherm constant (l/g), R is the gas constant (8.314 J/mol·K), and T is the Kelvin temperature (K).

16.5.3 Adsorption Kinetics

Adsorption kinetics was studied by Bayramoglu and Yilmaz (2018). Aljeboree et al. (2017) have described the pseudo-first-order and pseudo-second-order kinetics and equilibrium study for the adsorption of textile dyes on coconut shell activated carbon.

$$\log(q_e - q_t) = \log q_e - \frac{k_1 t}{2.303} \quad (6.15)$$

$$\frac{t}{q_t} = \frac{1}{k_2 q_e^2} + \frac{t}{q_e} \quad (6.16)$$

where q_t and q_e (mg/g) are adsorbed lead amount at time t (h) and equilibrium and k_1 (1/h) and k_2 (g/(mgh)) are the rate constant for the pseudo-first-order and pseudo-second-order adsorption kinetics, respectively.

Elovich equations

$$q_t = \left(\frac{1}{\beta} \right) \ln(\alpha\beta) + \left(\frac{1}{\beta} \right) \ln t \quad (6.17)$$

where q_e (mg/g) is the experimental amount of dye adsorbed at equilibrium and q_t (mg/g) is the amount of dye adsorbed at time t . For Elovich equations, α is the initial adsorption rate (mg/g/min), and the parameter β is related to the extent of surface coverage and activation energy for adsorption (g/mg).

16.5.4 Intraparticle Diffusion Model on Metal or Dye Adsorption

For most adsorption process, the amount of adsorption varies almost proportional with $t^{1/2}$.

$$q_t = K_{\text{diff}} t^{1/2} + C \quad (16.18)$$

where q_t is the adsorption capacity at time t , $t^{1/2}$ is the half-life time in second, and K_{diff} (mg/g min^{1/2}) is the rate constant of intraparticle diffusion.

To find out the rate constants, plot q_t versus $t^{1/2}$ gives a linear relationship, and K_{diff} can be determined from the slope of the plot.

Arrhenius equation is to determine the adsorption activation energy using the kinetic data. The kinetic constants (k) at each temperature are derived from the intraparticle diffusion models.

$$k = A e^{\left(-\frac{E_a}{RT}\right)} \quad (16.19)$$

$$\ln k = \ln A - \frac{E_a}{RT} \quad (16.20)$$

The adsorption activation energy is calculated by depicting $\ln(k)$ versus $1/T$.

A is the Arrhenius constant, R is the gas constant (8.314 J/mol K), E_a is the adsorption activation energy (J/mol), and T is temperature (K).

16.6 Characterization of Fungal Biosorbent

Several techniques are used for the characterization of fungal biosorbent, namely, ultraviolet (UV) spectroscopy, scanning electron microscopy (SEM), transmission electron microscopy (TEM), *energy dispersive X-ray spectroscopy* (EDX), Brunauer–Emmett–Teller (BET), Fourier-transform infrared spectroscopy (FTIR), Zeta potential analyzer, particle size analysis, and differential scanning calorimetry (DSC). Figure 16.9 shows the determination of the basic properties of an adsorbent by multifarious techniques.

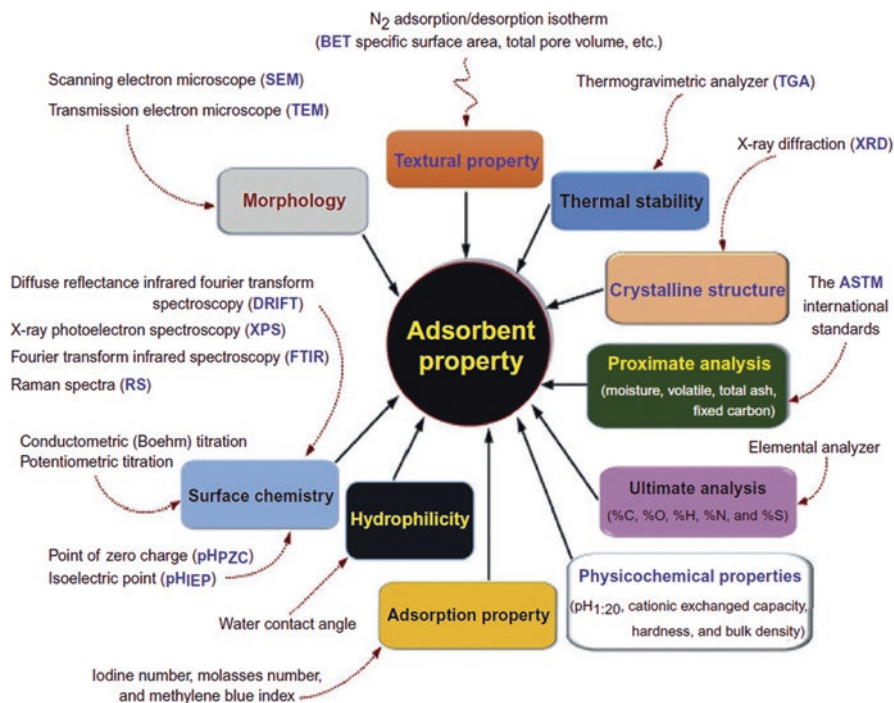


Fig. 16.9 Determination of the basic properties of an adsorbent by multifarious techniques (Unuabonah et al. 2019)

16.7 Adsorption Study

Adsorption studies are mainly done through batch and column study such as packed bed study.

16.7.1 Batch Adsorption Study

Adsorption of the heavy metals on fungal biomass is carried out in batch mode until equilibrium is established. The adsorption capacity of each metal ion adsorbed by the fungal biomass is determined (q_e , mmol g⁻¹) as the difference between their initial and final concentrations as given by Karunanayake et al. (2018) and Liu et al. (2018). Schematic diagram of batch biosorption equilibrium experimental procedure is represented in Fig. 16.10.

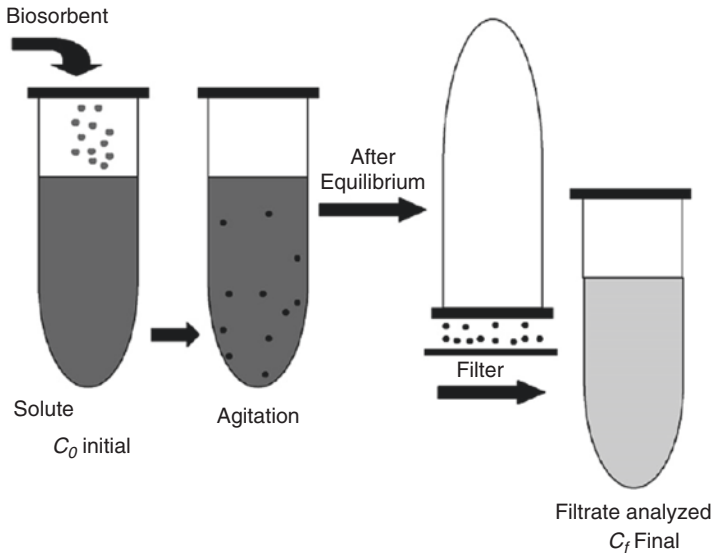


Fig. 16.10 Schematic diagram of batch biosorption equilibrium experimental procedure (Vijayaraghavan and Yun 2008)

$$Q_e = (C_0 - C_e) \times \frac{V}{m} \quad (16.21)$$

$$\text{Decolourization Rate (\%)} = \frac{C_0 - C_e}{C_0} \times 100\% \quad (16.22)$$

where C_0 and C_e (mg L^{-1}) are the initial and equilibrium concentrations after adsorption and Q_e (mg g^{-1}) is the equilibrium adsorption capacity. V (L) is the volume of acid dye solution, and m (g) is the mass of the adsorbents.

16.7.2 Column Adsorption Study

The fixed-bed column is made of a glass tube and packed with fungal biosorbent. The effluent samples are collected periodically from the bottom of the column during the experiment to determine the concentration of each collected sample (Fig. 16.11). A 45 mL of sample is placed in the Teflon liner with 4 mL of 15.9M HNO_3 and 1 mL of 12.1M HCl . The final extract was filtered through 0.45 μm syringe filter and analyzed using inductively coupled plasma mass spectrophotometry (ICP-MS) (Östman et al. 2017).

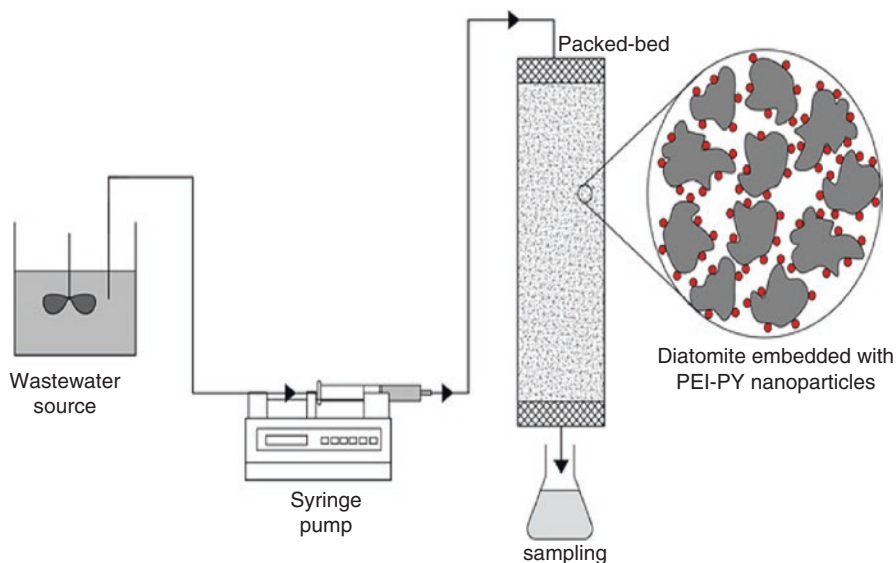


Fig. 16.11 Schematic representation of the fixed-bed experimental setup (Hethnawi et al. 2018)

16.7.3 Breakthrough Analysis

In the fixed-bed adsorption system, the breakthrough curve (BTC) behavior is affected by the operational parameters (i.e., Q , C_0 , Z , and % nps) and the designed parameters (length over diameter) of the column as well as the characteristic of the adsorbent (size and shape) (Fig. 16.12).

16.7.4 Packed Bed Column Model

Packed bed column is an effective process for cyclic sorption/desorption, as it makes the best use of the concentration difference known to be a driving force for pollutant sorption and results in a better quality of the effluent. Two frequently used models, i.e., Thomas and Bed Depth Service Time (BDST), were used to analyze the compatibility of experimental data of the tested metals.

16.7.4.1 Thomas Model

The Thomas model can be implemented to analyze the breakthrough curves and adsorption capacity for sorbent.

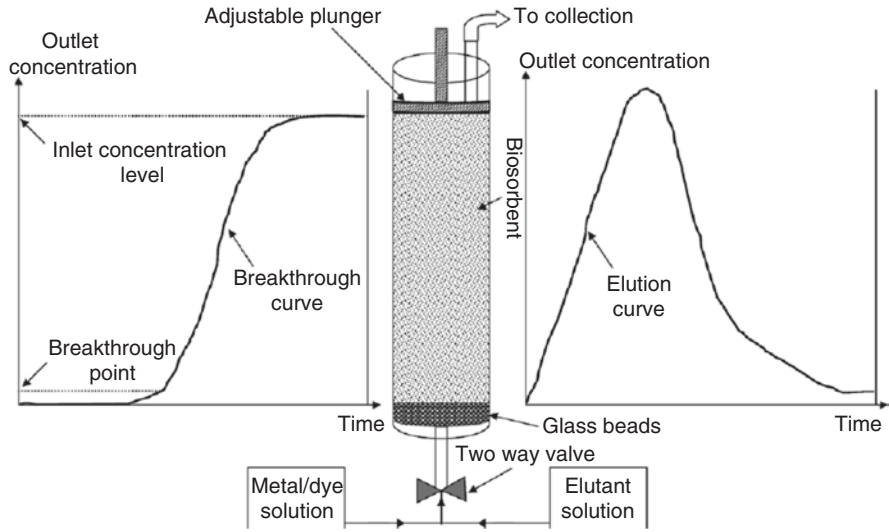


Fig. 16.12 Schematic diagram of packed column arrangement with biosorption breakthrough and elution curves (Vijayaraghavan and Yun 2008)

$$\ln\left(\frac{C_0}{C} - 1\right) = \frac{k_{Th} q_0 m}{Q} - k_{Th} C_0 t \tag{16.23}$$

where C_0 and C are the inlet and the effluent solute concentrations at any time t (m); k_{Th} is the Thomas model constant ($\text{mL m}^{-1} \text{mg}^{-1}$); q_0 is the maximum solid-phase concentration of solute (mg g^{-1}); and M is the total mass of the adsorbent (g).

The model constants k_{Th} and q_0 can be determined from slope and intercept of a plot of $\ln[(C_0/C) - 1]$ against t , respectively.

16.7.4.2 BDST Model

The BDST model is used to predict the column performance of any bed length, if data for some depths are known.

$$t = \frac{N_0 Z}{C_0 \vartheta} - \frac{1}{K_a C_0} \ln\left(\frac{C_0}{C_b} - 1\right) \tag{16.24}$$

where t is the service time (h), N_0 is the adsorption capacity (mg cm^{-3}), Z is the height of column (cm), C_b is the breakthrough sorbate concentration (mg L^{-1}), ϑ is the linear velocity (cm h^{-1}), and K_a is the rate constant ($\text{L mg}^{-1} \text{h}^{-1}$) at time t .

16.8 Validation of Adsorption Kinetics Models

The kinetic data was fit using the nonlinear form of the PFO and PSO models, where the best-fit was estimated by coefficient of determination (R^2) as validated by Jawad et al. (2019).

$$R^2 = 1 - \frac{\sum_{n=1}^{n=1} (q_{t,\text{meas}} - q_{t,\text{cal}})^2}{\sum_{N=1}^N (q_{t,\text{cal}} - \overline{q_{t,\text{cal}}})^2} \quad (16.25)$$

$q_{t,\text{meas}}$ and $q_{t,\text{cal}}$ are the measured and calculated adsorption capacity at time t , and n is the number of observations.

Chi-square and the normalized standard deviation are used to validate the kinetic models as cited by Inyinbor et al. (2016).

$$\chi^2 = \sum_n \frac{(q_{\text{exp}} - q_{\text{cal}})^2}{q_{\text{cal}}} \quad (16.26)$$

$$\Delta q_e (\%) = 100 \sqrt{\frac{(q_{\text{exp}} - q_{\text{cal}}) / q_{\text{exp}}}{N - 1}} \quad (16.27)$$

where N is the number of data points, while q_{exp} and q_{cal} are experimentally determined quantity adsorbed at equilibrium and calculated quantity adsorbed at equilibrium, respectively.

16.9 Factors Affecting Fungal Biosorption

Several factors affect the process of biosorption (Dhankhar and Hooda 2011; Arief et al. 2008; Bankar and Nagaraja 2018). Common factors are as follows:

- (i) Type and nature of biomass
- (ii) Initial solute concentration
- (iii) Biomass concentrations (biosorbent dose/solution volume) in solution
- (iv) Physicochemical factors like temperature, pH, and ionic strength

16.10 Factors Affecting Desorption

Numerous factors such as effect of desorption reagent, desorption temperature, and desorption time have been investigated by several researchers (Zhang and Wang 2015; Mahfoudhi and Boufi 2017). Desorption or recovery is an essential concept,

especially if the pH has an effect in the sustainable manner of adsorption study. But the regeneration process should not damage the adsorbent inside the fixed-bed column; otherwise, their reuse will be inefficient; 0.05 mM of HNO₃ at pH 5 can be used for desorption study.

$$\text{Desorption Efficiency (\%)} = \frac{q_{\text{de}}}{q_{\text{ad}}} \times 100 \quad (16.28)$$

where q_{de} is the quantity desorbed by each of the eluent and q_{ad} is the adsorbed quantity during loading.

16.11 Fungal Bioreactor for Wastewater Treatment

For the growth of fungus, different bioreactor configurations such as stirred tank reactor (STR), bubble column, airlift, and fluidized bed reactors are used. These reactors are used for wastewater treatment. Figure 16.13 shows fungal pellet reactor for removal of pollutants in wastewater, although batch reactors are also used for wastewater treatment (Espinosa-Ortiz et al. 2016).

- (i) *STR*: Stirred tank reactor is widely used for culturing fungal pellets and commonly used for removal of heavy metals and dyes during wastewater treatment.
- (ii) *Bubble column bioreactor*: Bubble column reactor belongs to the category of multiphase reactors, and it is advantageous for the use of fungal pellets to treat pollutants from wastewater.
- (iii) *Airlift bioreactor*: Airlift bioreactor is similar to bubble column bioreactor but contains draft tube which is always an internal or an external tube to improve circulation and oxygen transfer. It is used for wastewater treatment.
- (iv) *Fluidized bed reactor*: The fluidized bed reactor is characterized by its plug flow nature of fluid movement inside the reactor. The fluidization occurs when solid material (i.e., biomass) is suspended in an upward-flowing stream of fluid, which can be either liquid or gas. These reactors are used in wastewater treatment.

16.12 Conclusion and Future Prospects

Methods exist for wastewater treatment, but they have some disadvantages like chemical methods used chemicals that are threat to environment. Biological methods have advantages over chemical methods. Fungal biomass can be a novel inexpensive biosorbent for removal of heavy metals and dyes from aqueous solution. The structural arrangements of various functional groups collectively make fungal biomass a good biosorbent. Actually, the sorption (adsorption/absorption) is affected by interaction of waste material with functional groups of fungal biomass with various waste materials.

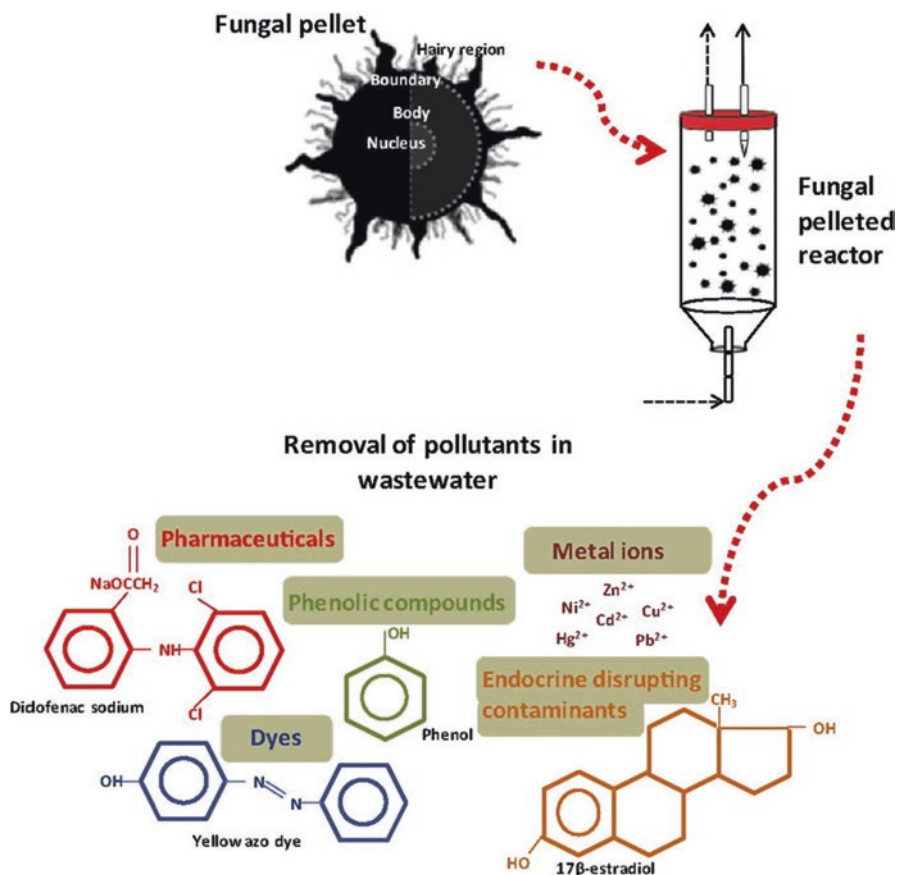


Fig. 16.13 Fungal pellet reactor for removal of pollutants in wastewater (Espinosa-Ortiz et al. 2016)

Acknowledgments The authors are thankful to the School of Bioengineering and Biosciences, Lovely Professional University, India, for providing library facilities.

References

- Aljeboree AM, Alshirifi AN, Alkaim AF (2017) Kinetics and equilibrium study for the adsorption of textile dyes on coconut shell activated carbon. *Arab J Chem* 10:S3381–S3393
- Antunes E, Jacob MV, Brodie G, Schneider PA (2017) Silver removal from aqueous solution by biochar produced from biosolids via microwave pyrolysis. *J Environ Manag* 203:264–272
- Arief VO, Trilestari K, Sunarso J, Indraswati N, Ismadji S (2008) Recent progress on biosorption of heavy metals from liquids using low cost biosorbents: characterization, biosorption parameters and mechanism studies. *CLEAN–Soil Air Water* 36(12):937–962
- Asgher M (2012) Biosorption of reactive dyes: a review. *Water Air Soil Pollut* 223(5):2417–2435

- Azimi A, Azari A, Rezakazemi M, Ansarpour M (2017) Removal of heavy metals from industrial wastewaters: a review. *Chem Bio Eng Rev* 4:37–59
- Bankar A, Nagaraja G (2018) Recent trends in biosorption of heavy metals by Actinobacteria. In: *New and future developments in microbial biotechnology and bioengineering*, (pp 257–275). Elsevier, Amsterdam, Netherland
- Bayramoglu G, Yilmaz M (2018) Azo dye removal using free and immobilized fungal biomasses: isotherms, kinetics and thermodynamic studies. *Fibers Polym* 19(4):877–886
- Burakov AE, Galunin EV, Burakova IV, Kucherova AE, Agarwal S, Tkachev AG, Gupta VK (2018) Adsorption of heavy metals on conventional and nanostructured materials for wastewater treatment purposes: a review. *Ecotoxicol Environ Saf* 148:702–712
- Couto SR (2009) Dye removal by immobilised fungi. *Biotechnol Adv* 27(3):227–235
- Crini G, Lichtfouse E, Wilson LD, Morin-Crini N (2018) Conventional and non-conventional adsorbents for wastewater treatment. *Environ Chem Lett* 17(1):195–213
- Dhankhar R, Hooda A (2011) Fungal biosorption—an alternative to meet the challenges of heavy metal pollution in aqueous solutions. *Environ Technol* 32(5):467–491
- Espinosa-Ortiz EJ, Rene ER, Pakshirajan K, van Hullebusch ED, Lens PN (2016) Fungal pelleted reactors in wastewater treatment: applications and perspectives. *Chem Eng J* 283:553–571
- Hegab HM, ElMekawy A, van den Akker B, Ginic-Markovic M, Saint C, Newcombe G, Pant D (2018) Innovative graphene microbial platforms for domestic wastewater treatment. *Rev Environ Sci Biotech* 17(1):147–158
- Hethnawi A, Manasrah AD, Vitale G, Nassar NN (2018) Fixed-bed column studies of total organic carbon removal from industrial wastewater by use of diatomite decorated with polyethylenimine-functionalized pyroxene nanoparticles. *J Colloid Interface Sci* 513:28–42
- Inyinbor AA, Adekola FA, Olatunji GA (2016) Kinetics, isotherms and thermodynamic modeling of liquid phase adsorption of Rhodamine B dye onto Raphiahookerie fruit epicarp. *Water Res Ind J* 15:14–27
- Jawad AH, Mamat NH, Hameed BH, Ismail K (2019) Biofilm of cross-linked Chitosan-Ethylene Glycol Diglycidyl Ether for removal of Reactive Red 120 and Methyl Orange: adsorption and mechanism studies. *J Environ Chem Eng* 7:102965
- Karunanayake AG, Todd OA, Crowley M, Ricchetti L, Pittman CU Jr, Anderson R, Mohan D, Mlsna T (2018) Lead and cadmium remediation using magnetized and nonmagnetized biochar from Douglas fir. *Chem Eng J* 331:480–491
- Kotrba P (2011) Microbial biosorption of metals—general introduction. In: *Microbial biosorption of metals*. Springer, Dordrecht, pp 1–6
- Kour D, Rana KL, Yadav N, Yadav AN, Rastegari AA, Singh C, Negi P, Singh K, Saxena AK (2019a) Technologies for Biofuel Production: current development, challenges, and future prospects. In: *Rastegari AA, Yadav AN, Gupta A (eds) Prospects of renewable bioprocessing in future energy systems*. Springer International Publishing, Cham, pp 1–50. https://doi.org/10.1007/978-3-030-14463-0_1
- Kour D, Rana KL, Yadav N, Yadav AN, Singh J, Rastegari AA, Saxena AK (2019b) Agriculturally and industrially important fungi: current developments and potential biotechnological applications. In: *Yadav AN, Singh S, Mishra S, Gupta A (eds) Recent advancement in white biotechnology through fungi, volume 2: perspective for value-added products and environments*. Springer International Publishing, Cham, pp 1–64. https://doi.org/10.1007/978-3-030-14846-1_1
- Kumari K, Abraham TE (2007) Biosorption of anionic textile dyes by nonviable biomass of fungi and yeast. *Bioresour Technol* 98(9):1704–1710
- Lei Y, Su H, Tian F (2018) A novel nitrogen enriched hydrochar adsorbents derived from salix biomass for Cr (VI) adsorption. *Sci Rep* 8:4040
- Li S, Huang J, Mao J, Zhang L, He C, Chen G, Parkin IP, Lai Y (2019) In vivo and in vitro efficient textile wastewater remediation by *Aspergillus niger* biosorbent. *Nanoscale Adv* 1(1):168–176
- Liu, X., Liu, M., & Zhang, L. (2018). Co-adsorption and sequential adsorption of the co-existence four heavy metal ions and three fluoroquinolones on the functionalized ferromagnetic 3D NiFe₂O₄ porous hollow microsphere. *Journal of colloid and interface science*, 511:135–144

- Lu F, Astruc D (2018) Nanomaterials for removal of toxic elements from water. *Coord Chem Rev* 356:147–164
- Madala S, Nadavala SK, Vudagandla S, Boddu VM, Abburi K (2017) Equilibrium, kinetics and thermodynamics of Cadmium (II) biosorption on to composite chitosan biosorbent. *Arab J Chem* 10:S1883–S1893
- Mahfoudhi N, Boufi S (2017) Nanocellulose: a challenging nanomaterial towards environment remediation. In: *Cellulose-reinforced nanofibre composites* (pp 277–304). Woodhead Publishing, Duxford, United Kingdom
- Marzougui Z, Damak M, Elleuch B, Elaissari A (2017) Occurrence and enhanced removal of heavy metals in industrial wastewater treatment plant using coagulation-flocculation process. In: *Euro-Mediterranean conference for environmental integration*. Springer, Cham, pp 535–538
- Masoudi R, Moghimi H, Azin E, Taheri RA (2018) Adsorption of cadmium from aqueous solutions by novel Fe₃O₄-newly isolated *Actinomyces* sp. bio-nanoadsorbent: functional group study. *Artif Cells Nanomed Biotechnol*, 46(sup3), S1092–S1101
- Nyairo WN, Eker YR, Kowenje C, Akin I, Bingol H, Tor A, Onger DM (2018) Efficient adsorption of lead (II) and copper (II) from aqueous phase using oxidized multiwalled carbon nanotubes/poly pyrrole composite. *Sep Sci Technol* 53(10):1498–1510
- Östman M, Lindberg RH, Fick J, Björn E, Tysklind M (2017) Screening of biocides, metals and antibiotics in Swedish sewage sludge and wastewater. *Water Res* 115:318–328
- Park CM, Chu KH, Her N, Jang M, Baalousha M, Heo J, Yoon Y (2017) Occurrence and removal of engineered nanoparticles in drinking water treatment and wastewater treatment processes. *Sep Purif Rev* 46:255–272
- Raghukumar S (2017) Fungi: characteristics and classification. In: *Fungi in coastal and oceanic marine ecosystems*. Springer, Cham, pp 1–15
- Rana KL, Kour D, Sheikh I, Dhiman A, Yadav N, Yadav AN, Rastegari AA, Singh K, Saxena AK (2019a) Endophytic fungi: biodiversity, ecological significance, and potential industrial applications. In: Yadav AN, Mishra S, Singh S, Gupta A (eds) *Recent advancement in white biotechnology through fungi: volume 1: diversity and enzymes perspectives*. Springer International Publishing, Cham, pp 1–62. https://doi.org/10.1007/978-3-030-10480-1_1
- Rana KL, Kour D, Sheikh I, Yadav N, Yadav AN, Kumar V, Singh BP, Dhaliwal HS, Saxena AK (2019b) Biodiversity of endophytic fungi from diverse niches and their biotechnological applications. In: Singh BP (ed) *Advances in endophytic fungal research: present status and future challenges*. Springer International Publishing, Cham, pp 105–144. https://doi.org/10.1007/978-3-030-03589-1_6
- Rastegari AA, Yadav AN, Gupta A (2019) *Prospects of renewable bioprocessing in future energy systems*. Springer International Publishing, Cham
- Stajich JE, Berbee ML, Blackwell M, Hibbett DS, James TY, Spatafora JW, Taylor JW (2009) Primer--the fungi. *Curr Biol* 19(18):R840
- Unuabonah EI, Omorogie MO, Oladoja NA (2019) Modeling in adsorption: fundamentals and applications. In: Kyzas GZ, Mitropoulos AC (eds) *Composite nanoadsorbents*. Elsevier, pp 85–118. <https://doi.org/10.1016/B978-0-12-814132-8.00005-8>
- Vijayaraghavan K, Yun Y-S (2008) Bacterial biosorbents and biosorption. *Biotechnol Adv* 26:266–291. <https://doi.org/10.1016/j.biotechadv.2008.02.002>
- Wang Y, Zhang W, Qin M, Zhao M, Zhang Y (2018) Green one-pot preparation of α -Fe₂O₃@carboxyl-functionalized yeast composite with high adsorption and catalysis properties for removal of methylene blue. *Surface Interface Anal* 50(3):311–320
- Yadav AN, Sachan SG, Verma P, Kaushik R, Saxena AK (2016) Cold active hydrolytic enzymes production by psychrotrophic Bacilli isolated from three sub-glacial lakes of NW Indian Himalayas. *J Basic Microbiol* 56:294–307
- Yadav A, Verma P, Kumar R, Kumar V, Kumar K (2017a) Current applications and future prospects of eco-friendly microbes. *EU Voice* 3:21–22
- Yadav AN, Kumar R, Kumar S, Kumar V, Sugitha T, Singh B, Chauhan V, Dhaliwal HS, Saxena AK (2017b) Beneficial microbiomes: biodiversity and potential biotechnological applications for sustainable agriculture and human health. *J Appl Biol Biotechnol* 5:45–57

- Yadav AN, Verma P, Kumar V, Sangwan P, Mishra S, Panjiar N, Gupta VK, Saxena AK (2018) Biodiversity of the genus *Penicillium* in different habitats. In: Gupta VK, Rodriguez-Couto S (eds) *New and future developments in microbial biotechnology and bioengineering*. *Penicillium* system properties and applications. Elsevier, Amsterdam, pp 3–18. <https://doi.org/10.1016/B978-0-444-63501-3.00001-6>
- Yadav AN, Mishra S, Singh S, Gupta A (2019a) *Recent advancement in white biotechnology through fungi Volume 1: diversity and enzymes perspectives*. Springer International Publishing, Cham
- Yadav AN, Mishra S, Singh S, Gupta A (2019b) *Recent advancement in white biotechnology through fungi. Volume 2: perspective for value-added products and environments*. Springer International Publishing, Cham
- Yagub MT, Sen TK, Afroze S, Ang HM (2014) Dye and its removal from aqueous solution by adsorption: a review. *Adv Colloid Interface Sci* 209:172–184
- Yao ZY, Qi JH, Wang LH (2010) Equilibrium, kinetic and thermodynamic studies on the biosorption of Cu (II) onto chestnut shell. *J Hazard Mat* 174:137–143
- Yin K, Wang Q, Lv M, Chen L (2018) Microorganism remediation strategies towards heavy metals. *Chem Eng J* 360:1153–1563
- Zhang X, Wang X (2015) Adsorption and desorption of nickel (II) ions from aqueous solution by a lignocellulose/montmorillonite nanocomposite. *PLoS One* 10:e0117077
- Zhu W, Lei J, Li Y, Dai L, Chen T, Bai X, Wang L, Duan T (2019) Procedural growth of fungal hyphae/Fe₃O₄/graphene oxide as ordered-structure composites for water purification. *Chem Eng J* 355:777–783